Utilizing Synchrophasor-Based Protection Systems with VSC-HVDC Controls to Mitigate Voltage Instability

Rujiroj Leelaruji, *Student Member, IEEE* and Luigi Vanfretti, *Member, IEEE*

***Abstract*—This article rationalizes the need of coordination between protective systems and VSC-HVDC controls to steer power systems away from voltage instability conditions. The concept of coordination involves the use of feasible communication mechanisms which can be exploited by protection systems to send out a "protective information set" to an algorithm which will determine preventive, corrective, and protective actions particularly by taking advantage of the availability of VSC-HVDC. This "protective information set" considers synchrophasor vector processing capabilities which allows for the exploitation of phasor measurements while satisfying protective relaying data transmission and processing requirements. Coordination refers to the ability of the protective systems and VSC-HVDCs to cooperate and to synchronize their actions so that voltage instability can be avoided.**

***Index Terms*—Wide Area Monitoring, Protection and Control, Synchrophasor applications, Wide-Area Voltage Instability Detection, Wide-Area Early Warning Systems, VSC-HVDC.**

I. Introduction

The technology behind Phasor Measurement Units (PMUs) can be traced back to the computer relaying field. The marriage of PMU and relay technology has lead to the inception of a revolutionary field in power system protection, in which this microprocessors technology is no longer only designed to fulfill protection purposes. This technology now also considers the communication mechanisms allowing the transmission of synchronized phasor measurement, now one of the features available in the most advanced protective relays commercially available, and the use of this feature in protection applications is proliferating [1]. As a result, the Wide-Area Monitoring, Protection and Control System (WAMPAC) built on synchrophasor capabilities are being used in many applications such as in the synchronization distributed generation to large power grids [2] or for the integration of distributed renewable sources of energy [3].

Simultaneously, technological advances in Voltage Source Converters-based High Voltage Direct Current (VSC-HVDC) have allowed to prove this technology's advantages for control, such as the ability to independently control active and reactive [4] and voltage control. These controllable devices are considered to be promising devices that can improve the performance and reliability of power systems. Some applications which combines the WAMS and control of VSC-HVDC have been implemented, for instance WAMS with embedded VSC-HVDC control for oscillation damping [5]. This suggests that VSC-HVDCs with properly designed control strategies exploiting synchrophasor data from protection systems can substantially mitigate power system voltage instability. This concept is investigated in this article.

The remainder of this article is structured as follows. Section II offers a synthesis of wide-area voltage stability monitoring concepts, while the proposed coordination between protection systems and VSC-HVDC is described in Section III. Section IV presents the different control strategies of VSC-HVDC to mitigate voltage instability. Finally, in Section V, conclusions are drawn and future work is outlined.

Manuscript submitted to the IEEE PES International Conference on Power Systems Technology (POWERCON), October 30 - November 2, 2012, Auckland, New Zealand.

The authors are with the Electric Power Systems Division, School of Electrical Engineering, KTH Royal Institute of Technology, Teknikringen 33, SE-100 44, Stockholm, Sweden. E-mail: rujiroj@kth.se, luigiv@kth.se

II. Wide-Area Voltage Stability Monitoring

PMUs have been adopted to implement applications for Wide-Area Monitoring, Control and Protection (WAMPAC) Systems or Wide-Area Monitoring Systems (WAMS) which can be found in [6] and [7], respectively. The use of these applications is catered, for example, to provide the wide-area visibility [8], the detection of critical oscillatory mode properties [9], and voltage instability detection [10]. To have an overall situation awareness for voltage instability detection applications, it appears that the entire power system state needs to be reconstructed from synchrophasor measurements and other data [11], or that different indices for different system components need to be computed to determine instabilities [12].

For voltage stability monitoring, the authors propose to track the sensitivities of a Jacobian matrix, similarly to the approach in [13][1]. The elements in a modified Jacobian matrix (2) are derived from the power flow in each transmission line. This means that the effects of shunt capacitances of the transmission line (in the case of medium and short lines) of the nominal π-model are also included.

The transmitted power on the line can be expressed as follows:

$$\begin{aligned} \overline{S}_{ik} &= V_i e^{j\delta_i}\{I_{ik}e^{j\delta_{ik}}\}^* \\ P_{ik} &= Re(\overline{S}_{ik}), \quad Q_{ik} = Im(\overline{S}_{ik}) \end{aligned} \tag{1}$$

where
V_i = voltage magnitude at Bus i.
I_{ik} = current magnitude from from Bus i to Bus k.
δ_i = voltage angle at Bus i.
$\delta_{ik} = \delta_i - \delta_k$.
$\overline{S}_{ik}$ = complex power transmitted from Bus i to Bus k.
P_{ik} = transmitted real power from Bus i to Bus k.
Q_{ik} = transmitted reactive power from Bus i to Bus k.

From (1) it follows that the real and reactive power flows through the transmission lines can be calculated directly

[1] Observe that this is not the same Jacobian matrix as in the standard power flow problem where each element is related to an injected power to the bus

978-1-4673-2868-5/12/$31.00 ©2012 IEEE

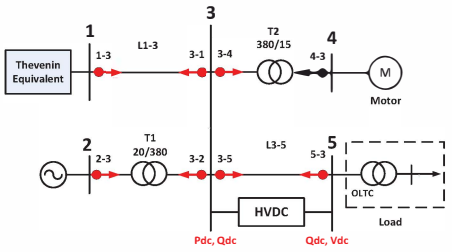

Fig. 1. Test system used for generating voltage instability scenarios

from the measured voltage and current phasors regardless the system's parameters.

The modified Jacobian matrix can be constructed as follows:

$$J(\delta, V) = \begin{bmatrix} P_{ik_\delta}(t) & P_{ik_V}(t) \\ Q_{ik_\delta}(t) & Q_{ik_V}(t) \end{bmatrix} \quad (2)$$

where

$P_{ik_\delta}(t) = P_{ik}(t) - P_{ik}(t-1)/\delta_i(t) - \delta_i(t-1) = dP_{ik}/d\delta_i$

$P_{ik_V}(t) = P_{ik}(t) - P_{ik}(t-1)/V_i(t) - V_i(t-1) = dP_{ik}/dV_i$

Similar expressions can also be derived for Q_δ and Q_V.

The values of these sensitivities can aid in assessing voltage instability with the considerations below.

1) The sensitivities are consistently at a low-positive value[2] with the assumption of steady-state operation. This indicates operation away from a voltage instability condition.
2) The value of the sensitivities will increase positively (or negatively) when a system is stressed. This denotes a system is moving towards a "weak" operating condition, this is a trend in the development of the voltage instability.
3) The value increases abruptly to very high positive (or negative) and switches sign in the case of a lack of reactive power support for dV_i/dQ_{ik} or when the maximum power transfer is reached for dV_i/dP_{ik}. This depicts an unstable condition which consequently leads to voltage collapse.

However, before computing sensitivities, the original voltages phasors must be filtered to remove fast dynamics and large outliers. Moreover, a moving average (MA) filter aids to increase the robustness of the computed sensitivities. However, these filtering methods (either with or without moving average window) introduce a small delay to the calculation of sensitivities. More details regarding this filtering approach can be found in [14]. In addition, only dV_i/dP_{ik}, and dV_i/dQ_{ik} are studied and used as voltage instability indicators in this paper.

To illustrate, a voltage instability scenario is conducted by gradually increasing constant active and reactive load models at Bus 5 of the test system shown in Fig. 1. A load with constant power characteristics with an automatic discrete on-load tap changer (OLTC) dynamics at the distribution side are explicitly modelled at Bus 5. Details of generator model in this system can be found in [15]. Bus 3-to-Bus 5 transfers are considered here when the Bus 3 HVDC terminal is a rectifier.

[2]Or negative depending the current measurement direction.

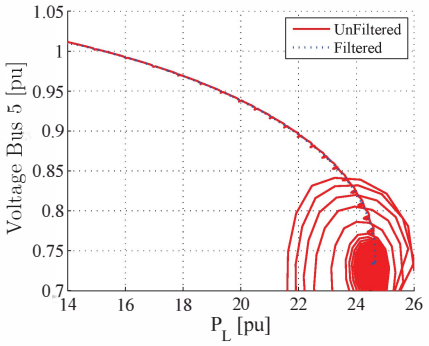

(a) PV-curve (Load Power vs Voltage Bus 5)

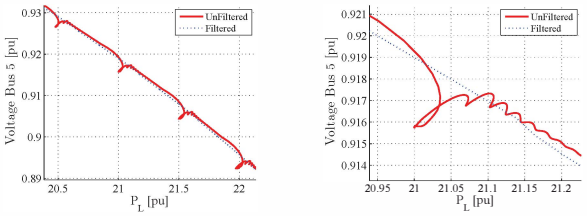

(b) Zoom of Fig. 2a (c) Zoom of Fig. 2b

Fig. 2. An example of filtered and unfiltered PV-curves.

Fig. 2 shows PV-curve (Load power vs. Voltage at Bus 5) resulting from the load increase which is assumed to change as follows:

$$\begin{aligned} P_L &= P_{Lo}(1+\lambda) \\ Q_L &= Q_{Lo}(1+\lambda) \end{aligned} \quad (3)$$

where P_{Lo} and Q_{Lo} are the initial base active and reactive powers, respectively, and λ is a varying parameter representing the loading factor. Fig. 3a and 3b depict the corresponding sensitivities (dV_5/dP_{53} and dV_5/dQ_{53}) calculated from unfiltered, filtered, filtered with MA, respectively.

As seen from Fig. 2 to 3b, filtering approach plays a vital role. A lack of and/or incorrect data processing can yield in incorrect information, which can result in an improper control action, which in turn could lead to a collapse. The spikes shown in the green in Fig. 3 correspond to OLTC tap position changes. It can also be noted that the sensitivity calculated from the unfiltered data (green dashed line) are vulnerable to OLTC tap switching and vary abruptly compared with those computed using data which has been filtered, or filtered with MA.

In addition, the sensitivities can be used to generate an early warning alarm when its value changes from positive to negative. This early warning alarm can be generated by setting a threshold value (which is pre-set through stability studies), allowing instability detection before the sensitivity changes abruptly to a large positive value. The horizontal yellow and red dash-dot lines in Fig. 3 indicate an insecure and an emergency state, that have been pre-set, respectively. Fig. 4 illustrates PV and QV-curve plots of active and reactive load vs. the voltage at Bus 5 with zero DC power (plotted from filtered data).

As seen in Fig. 4, it is clear that the bifurcation point of both curves can occur at different times, thus it is necessary

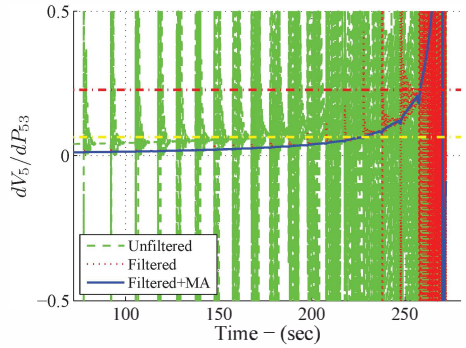

(a) dV_5/dP_{53}

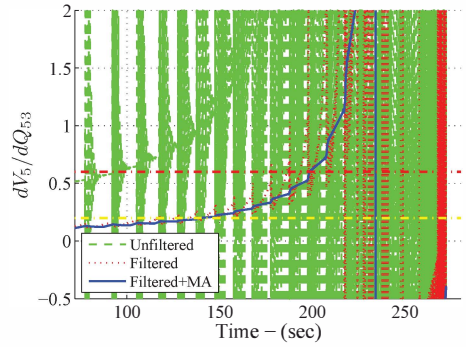

(b) dV_5/dQ_{53}

Fig. 3. Plot of calculated dV_5/dP_{53} and dV_5/dQ_{53} sensitivity calculated from filtered and unfiltered signals.

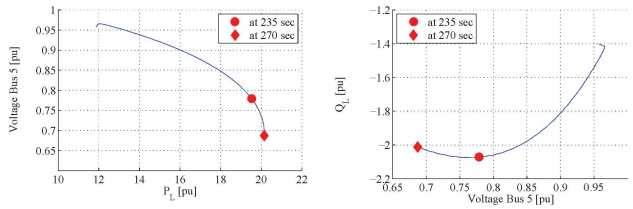

(a) $PV-curve$ (b) $QV-curve$

Fig. 4. Plot of calculated $PV-curve$ and $QV-curve$ calculated from filtered signals.

to track both dV_i/dP_{ik} and dV_i/dQ_{ik}sensitivities. Moreover, these bifurcation points in $PV-curve$ and $QV-curve$ implicitly correspond to the change of sensitivities as shown in Fig. 3. Therefore, early warnings and final alarms regarding active and reactive power problem are recommended to set in different values. For instance, two thresholds for alarms are set at dV_5/dP_{53} = 0.08 and dV_5/dQ_{53} = 0.2, for an early warning signal (yellow dash-dot line), and dV_5/dP_{53} = 0.24 and dV_5/dQ_{53} = 0.6, for a final alarm (red dash-dot line), respectively.

III. Coordination of Synchrophasor-based Protection System and VSC-HVDC

In previous simulation studies [14] it has been illustrated how the bifurcation points of the $PV-curve$ and $QV-curve$ can also occur at the instant. This can be done by varying λ in (3) at a different rate. However, it is more important to mention that only the reactive power sensitivity dV_5/dQ_{53}, and the active power sensitivity dV_5/dP_{53} in both studies experience the abrupt change in their values as discussed above. This means that the problematic location that tends toward voltage instability regarding reactive power is at point *5-3*, while points *3-5* and *5-3* shown in Fig. 1 need to be considered for active power issues. To avoid the repetition of results and present new experiments, the computed sensitivities at other locations are omitted. In order to mitigate voltage instability, an early warning signal can be adopted to trigger the change of power transfer though an VSC-HVDC. Fig. 5 shows a block diagram of the proposed method to adapt the HVDC control.

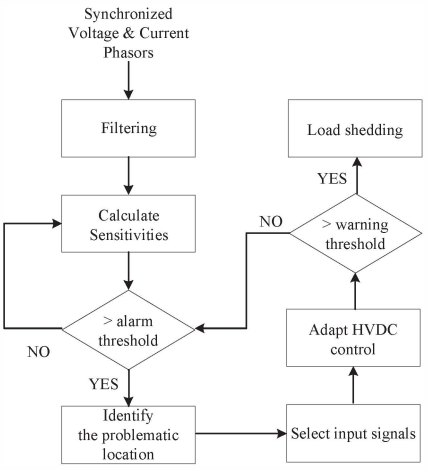

Fig. 5. Proposed method to mitigate voltage instability

As seen from Fig. 5, the method starts by gathering synchronized voltage and current phasors from different locations (see the 'red-dot' trace in Fig. 1). Then, these phasors are used to computed sensitivities as described in (1) and (2). Next, the computed sensitivities (dV_i/dP_{ik} and dV_i/dQ_{ik}) are compared with pre-set values of early warning signals to determine the locations leading to voltage instability. After problematic locations have been found, system quantities are selected as input signals to change the control mode and/or operational reference of the VSC-HVDC. The VSC-HVDC that is used in this article is the built-in model available from the PowerFactory [16] software's library. The original model is modified by implementing the additional PI-controller (indicated by dash box in Fig. 6) to change the active and reactive reference power of the VSC-HVDC . In the case of reactive power, the input signal of this PI-controller is the measured voltage level of the problematic location indicated by computed sensitivities while the voltage reference value (U_{ss} in Fig. 6a) is the voltage value when an early warning is triggered. In case of active power, the input signals (in this paper) are measured voltage angles at bus 3 and 5 (which are selected w.r.t. the sensitivities dV_5/dP_{53} mentioned earlier), while the angle reference value (θ_{ss} in Fig. 6b) is the angle different between bus 3 and bus 5 when an early warning is triggered.

Finally, if sensitivities approach values near the final alarms, a load shedding scheme has to be activated to disconnect loads.

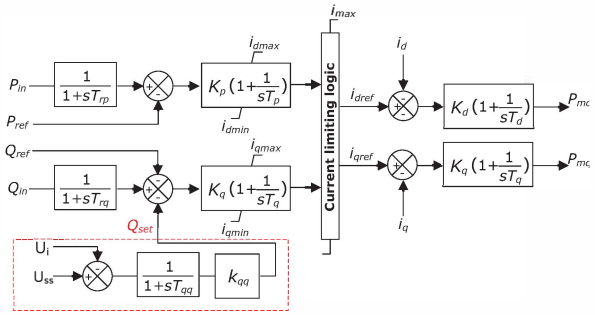

(a) Control Scheme for Inverter (Bus 5)

(b) Control Scheme for Rectifier (Bus 3)

Fig. 6. Control Scheme for VSC-HVDC

In this article, the load shedding scheme is only prevents the load increase, load shedding strategies can be found in [17]. In addition, parameters for the PI-controller such as gain and time constant values are selected regardless of particular response characteristics of the VSC-HVDC. Different controller parameters can provide different rise time, overshoot, time-to-peak, or steady-state error respecting the same physical limits of VSC-HVDC. This paper only focuses on how to utilize sensitivities in order to mitigate voltage collapse. The important issue of control tuning will be addressed in a future publication.

IV. Case Studies

In this section we present simulation results that illustrate the test system's response with and without the inclusion of our purposed method as shown in Fig. 5. In these simulations we have considered the load increase as the system perturbation which could lead to voltage instability, different power responses supported by the VSC-HVDC, and also different control modes at inverter side are included. The control at the rectifier side is $P_{dc} - Q_{dc}$ mode where the active and reactive power are fixed at 400 MW and 10 MVar (where each converter size is 550 MVA), respectively. Meanwhile, the active and reactive load are 1500 MW and 150 MVar and being increased (at t = 1 sec) as explained in (3) until test system experience voltage collapse.

A. Case 1: $Q_{dc} - V_{dc}$: Ramp support Q_{dc}

In this case, reactive power support at the inverter side is ramped up. This reactive power ramping is achieved through the control scheme shown in Fig. 6a. The comparison of the resulting PV and QV-curves with and without reactive power ramping is shown in Fig. 7. Meanwhile, the comparison of voltage at Bus 5 between with and without reactive ramping cases is shown in Fig. 8.

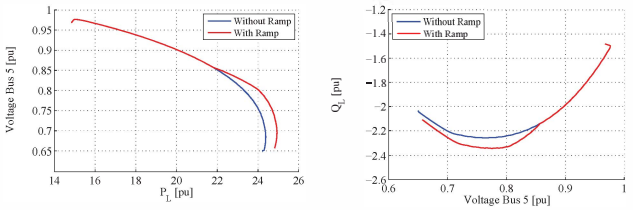

(a) $PV - curve$ (b) $QV - curve$

Fig. 7. $PV - curve$ and $QV - curve$ plots of Case 1

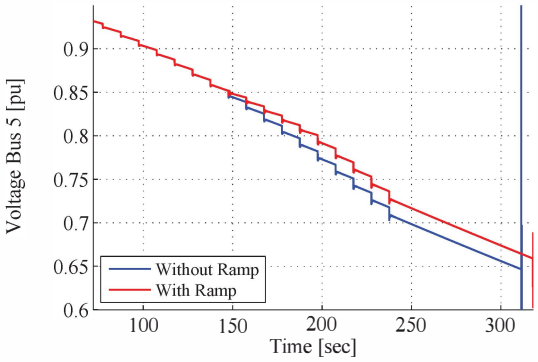

Fig. 8. Voltage at Bus 5 comparison between with and without VSC-HVDC coordination

As shown in Fig. 8, the reactive power that is ramped up by VSC-HVDC supports a voltage drop caused by increasing load. This voltage support allows the system to operate 10 more seconds before a collapse.

For comparison, the following schemes have been considered to control: reactive power Case 1), active power (Case 2), and both active and reactive power (Case 3) are ramped in such a way that make a test system collapses at approximately same point (see Fig. 8). Fig. 9 shows the delay of an abrupt change of sensitivities compared to the case without control.

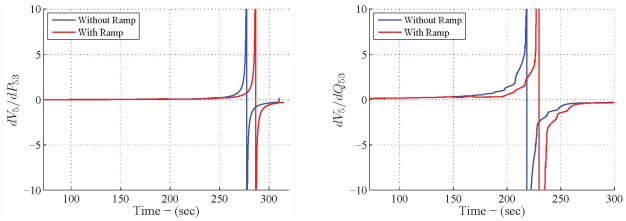

(a) dV_5/dP_{53} (b) dV_5/dQ_{53}

Fig. 9. dV_5/dP_{53} and dV_5/dQ_{53} sensitivities comparison between with and without VSC-HVDC coordination

B. Case 2: $Q_{dc} - V_{dc}$: Ramp support P_{dc}

This case is similar to Case 1, however despite the reactive power support at inverter side, active power is ramped up

at rectifier side and transmitted through DC line. The active power ramping is controlled through the scheme shown in Fig. 6b. Meanwhile, Fig. 10 shows the comparison of PV-curve and QV-curve between with and without active power ramping.

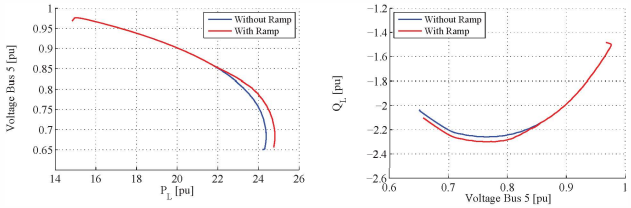

(a) $PV-curve$ (b) $QV-curve$

Fig. 10. $PV-curve$ and $QV-curve$ plots of Case 2

The increase of active power load is allowed to flow through the VSC-HVDC, resulting in a decrease of active power transfer through the parallel AC transmission line, L3-5. By transmitting higher power through VSC-HVDC, the system AC stress is relieved, loadability is increased and lower electrical losses occur. The system's loadability represented by PV and QV-curves are greater than in the case without active power ramping.

C. Case 3: $Q_{dc} - V_{dc}$: Ramp support P_{dc} & Q_{dc}

In this case, the active power support (P_{dc}) is ramped up by the rectifier while the reactive power Q_{dc} is ramped up by inverter. This means that we take advantages of VSC-HVDC described in both Case 1 and Case 2 to extend the maximum power transfer (MPT) point before the test system confronts voltage instability. Fig. 11 shows the comparison of PV and QV-curves between only Q_{dc} ramping (Case 1), only P_{dc} ramping (Case 2), and P_{dc} & Q_{dc} (Case 3) ramping. These associated PV and QV-curve shows three different ways to utilize the capacity of the VSC-HVDC. It cam be seen that, ramping both active and reactive power by VSC-HVDC provides the best loadability in the system. Table I shows a comparison between all three control schemes.

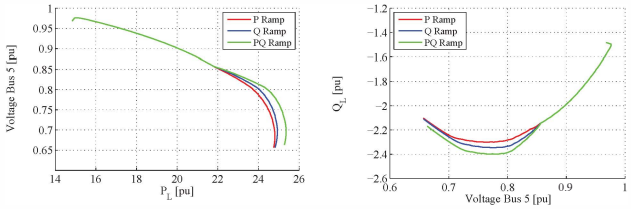

(a) $PV-curve$ (b) $QV-curve$

Fig. 11. Comparison of $PV-curve$ and $QV-curve$ plots between Case 1, 2, and 3

D. Case 4: $Q_{dc} - V_{dc}$: Step support P_{dc}

This case is similar to Case 2 in which the VSC-HVDC supports only active power. However, instead of ramping active power, the transmitted power is controlled through a step response. It is worth noting that since HVDC's operation depends on alarms that are set by the user, examples of stepping up DC power at different sensitivity values (which corresponds to different in time) are important to analyse. Fig. 12 shows the upper half of PV curves considering the AC flows through line L3-5 vs. the voltage at Bus 3 and the DC active power increase in a step change from 400 MW to 550 MW at the HVDC.

TABLE I
LOADABILITY OF DIFFERENT CONTROL SCHEMES

Control	MPT [p.u.]	Gain [p.u.]	Gain/Converter Size
No Control	24.38	-	-
P_{dc} Control	24.81	0.43	-21 %
Q_{dc} Control	24.98	0.60	+9 %
P_{dc} & Q_{dc} Control	25.36	0.98	+78 %

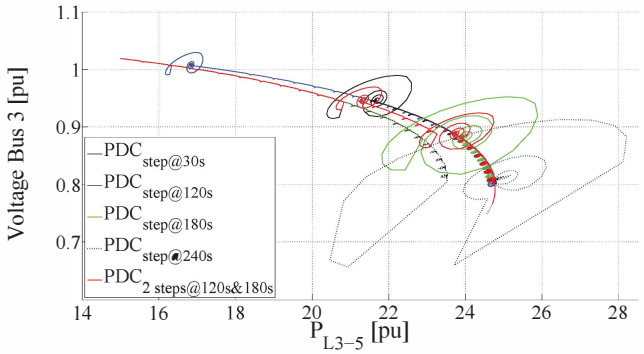

Fig. 12. PV-curves from unfiltered data - Step DC

From Fig. 12, it can be noting that setting alarms also plays a vital role in finding new power system's equilibrium, i.e. operational point. Observe that an early adjustment of the DC transfer results in a shorter settling time, and that if adjustments are made latter, the use of 2 different stages in the transition can aid in reducing the overshoot and settling time required for finding a new equilibrium. Moreover, a step change of DC power creates oscillations in the system's response, thus the DC power should be gradually changed to prevent this undesired feature. For comparison, Fig. 13 shows the PV-curve from unfiltered data in case of ramping DC power.

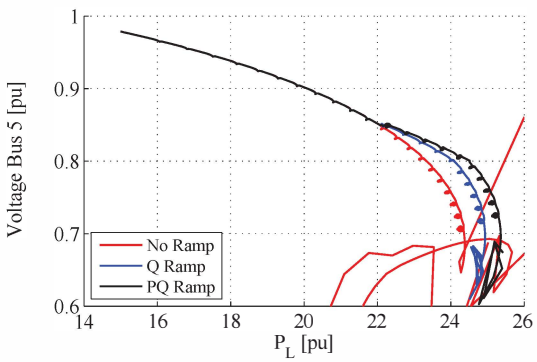

Fig. 13. PV-curves from unfiltered data - Ramp DC

E. Case 5: P_{dc} & V_{ac} at inverter

It has been noted before that Bus 5 experiences voltage stability issues, thus the control of inverter is changed from $Q_{dc} - V_{dc}$ to $P_{dc} - V_{ac}$ mode to investigate control schemes' efficiency. However, in order to keep the active power on the AC side to be equal to the active power transmitted from the DC side (losses neglected), the control mode of the other side must control the DC voltage [18]. Therefore the control mode of the rectifier is changed to $V_{ac} - V_{dc}$ mode. Fig. 14 shows a comparison of the PV-curves between no ramping, PQ ramping (Case 3), and AC voltage control at Bus 5.

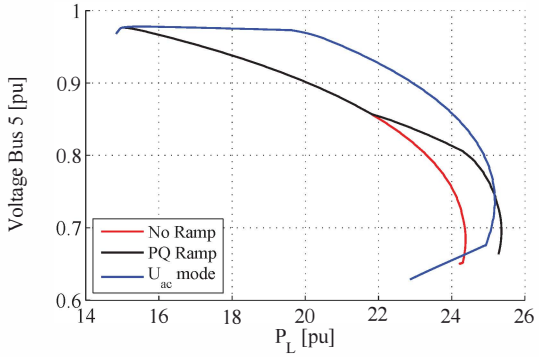

Fig. 14. Comparison of PV-curves between different control modes

As shown in Fig. 14, the voltage at Bus 5 is kept constant in the case of AC voltage control. This is because reactive power is injected from the inverter of the VSC-HVDC. However the voltage cannot be held any longer when active load power increases to 20 p.u. due to the VSC-HVDC's inner current control reaching its limit. Consequently, voltage at Bus 5 starts declining until system collapse. It is worth noting that the proposed control scheme (ramping active and reactive power) provides a better result as can be seen from the MTP point between these two cases.

V. Conclusions and Future Work

This article has described an approach for exploiting voltage sensitivities computed from synchrophasor data for wide-area voltage stability monitoring. This "monitoring tool" can be used to track the state of a power system during normal and severe operating conditions. The idea behind this approach is not only to use these sensitivities for monitoring purposes but also to automatically generate early warning signals before a collapse occurs. Different stress conditions are determined by the value of the sensitivities which need to be computed from filtered synchrophasor measurement data. The filtering approach has a large impact in sorting out unwanted electromechanical oscillations, noise and outliers before computing the sensitivities.

To utilize the computed sensitivities for mitigating voltage instabilities, several control schemes are developed for an VSC-HVDC which operates in parallel with an AC transmission line. The controls are implemented additionally to the standard control schemes of VSC-HVDC in order to change its operating set point. Simulations of different controls confirm the benefits of using these controls in a VSC-HVDC connected in parallel with an AC line for voltage support and better power flow management, with implicit considerations of the VSC-HVDC's size.

There are several issues that must be further addressed, including but not limited to: validation of the control schemes with different voltage instability scenarios, tuning parameters of the additional PI-controller properly, optimization of mixed control (P_{dc} & Q_{dc}), among others. The ultimate goal is not only to prevent long-term voltage instability, but also to use these sensitivities wisely so to mitigate all range of voltage instabilities that are generated by certain controls such as over and/or under-excitation limiters.

References

[1] E. Schweitzer, D. Whitehead, and G. Zweigle, "Real-world synchrophasor solutions," in *IEEE Power & Energy Society General Meeting*, 2009.

[2] R. Best, D. Morrow, D. Laverty, and P. Crossley, "Synchrophasor Broadcast Over Internet Protocol for Distributed Generator Synchronization," *IEEE Transactions on Power Delivery*, vol. 25, no. 4, pp. 2835 –2841, oct. 2010.

[3] D. Laverty, D. Morrow, R. Best, and P. Crossley, "Differential rocof relay for loss-of-mains protection of renewable generation using phasor measurement over internet protocol," in *Integration of Wide-Scale Renewable Resources Into the Power Delivery System, 2009 CIGRÉ/IEEE PES Joint Symposium*, july 2009.

[4] L. Zhang, L. Harnefors, and P. Rey, "Power system reliability and transfer capability improvement by vsc-hvdc," in *CIGRÉ Regional Meeting*, June 2007.

[5] J. Pan, R. Nuqui, K. Srivastava, P. Holmberg, and Y. Hafner, "AC Grid with Embedded VSC-HVDC for Secure and Efficient Power Delivery," in *IEEE Energy 2030 Conference*, 2008.

[6] V. Terzija, G. Valverde, D. Cai, P. Regulski, V. Madani, J. Fitch, S. Skok, M. Begovic, and A. Phadke, "Wide-Area Monitoring, Protection, and Control of Future Electric Power Networks," *Proceedings of the IEEE*, vol. 99, no. 1, pp. 80 –93, jan. 2011.

[7] J. Hauer and J. DeSteese, "Descriptive Model of Generic WAMS," Pacific Northwest National Laboratory,Richland, WA., Tech. Rep., 2007.

[8] Y. Zhang, P. Markham, T. Xia, L. Chen, Y. Ye, Z. Wu, Z. Yuan, L. Wang, J. Bank, J. Burgett, R. Conners, and Y. Liu, "Wide-Area Frequency Monitoring Network (FNET) Architecture and Applications," *IEEE Transactions on Smart Grid*, vol. 1, no. 2, pp. 159–167, Sept 2010.

[9] A. Hauer, D. Trudnowski, and J. DeSteese, "A Perspective on WAMS Analysis Tools for Tracking of Oscillatory Dynamics," in *IEEE Power Engineering Society General Meeting*, 2007, pp. 1–10, dOI: 10.1109/PES.2007.386186.

[10] M. Parashar and J. Mo, "Real Time Dynamics Monitoring System (RTDMS): Phasor Applications for the Control Room," in *42nd Hawaii International Conference on System Sciences, 2009 (HICSS '09)*, Jan 2009.

[11] M. Glavic and T. Van Cutsem, "Investigating state reconstruction from scarce synchronized phasor measurements," in *2011 IEEE Trondheim PowerTech*, 2011.

[12] B. Milosevic and M. Begovic, "Voltage Stability Protection and Control using a Wide-Area Network of Phasor Measurements," *IEEE Transactions on Power Systems*, vol. 18, pp. 121–127, 2003.

[13] M. Glavic and T. Van Cutsem, "Wide-Area Detection of Voltage Instability From Synchronized Phasor Measurements. Part I: Principle," *IEEE Transactions on Power Systems*, vol. 24, pp. 1408 – 1416, 2009.

[14] R. Leelaruji, L. Vanfretti, and M.S. Almas, "Voltage Stability Monitoring using Sensitivities Computed from Synchronized Phasor Measurement Data," in *accepted for publication, IEEE PES General Meeting 2012*, july 2012.

[15] R. Leelaruji and L. Vanfretti, "Detailed modelling, implementation and simulation of an "all-in-one" stability test system including power system protective devices," *Simulation Modelling Practice and Theory*, vol. 23, pp. 36 – 59, April 2012.

[16] *DIgSILENT PowerFactory Version 14*. [Online]. Available: http://www.digsilent.de/

[17] C. Taylor, "Concepts of undervoltage load shedding for voltage stability," *IEEE Transactions on Power Delivery*, vol. 7, pp. 480 – 488, April 1992.

[18] C. Du, "Vsc-hvdc for industrail power systems," Ph.D. dissertation, Chalmers University of Technology, 2007.